HHS Public Access

Author manuscript

J Neuroimaging. Author manuscript; available in PMC 2019 November 01.

Published in final edited form as:

J Neuroimaging. 2018 November ; 28(6): 615–620. doi:10.1111/jon.12546.

REAL-TIME CEREBRAL HEMODYNAMIC RESPONSE TO TACTILE SOMATOSENSORY STIMULATION

Benjamin Hage, M.S.[1], **Emily Way, B.S.**[1], **Steven M. Barlow, Ph.D.**[1,2], and **Gregory R. Bashford, Ph.D., P.E.**[1]

[1]Department of Biological Systems Engineering, University of Nebraska-Lincoln

[2]Department of Special Education and Communication Disorders, University of Nebraska-Lincoln

Abstract

Background and Purpose—Recent studies in rodents suggest somatosensory stimulation could provide neuroprotection during ischemic stroke by inducing plasticity in the cortex-vasculature relationship. While functional MRI (fMRI) has shown that somatosensory stimulation increases cerebral blood flow over several seconds, sub-second changes in cerebral blood flow in the basal cerebral arteries have rarely been studied due to temporal resolution limitations. This study characterized hemodynamic changes in the middle cerebral arteries (MCAs) during somatosensory stimulation with high temporal resolution (100 samples/sec) using functional transcranial Doppler ultrasound (fTCD).

Methods—Pneumotactile somatosensory stimulation, consisting of punctate pressure pulses traversing the glabrous skin of the hand at 25 cm/s, was used to induce cerebral blood flow velocity (CBFV) response curves. Changes in CBFV were measured in the bilateral MCAs using fTCD. All 12 subjects underwent three consecutive trials consisting of 20 s of stimulation followed by 5 min of rest.

Results—Sharp, bilateral increases in CBFV of about 20% (left MCA = 20.5%, right MCA = 18.8%) and sharp decreases in pulsatility index of about 8% were observed during stimulation. Left lateralization of up to 3.9% was also observed. The magnitude of the initial increase in CBFV showed significant adaptation between subsequent trials.

Conclusions—Pneumotactile somatosensory stimulation is a potent stimulus which can evoke large, rapid hemodynamic changes, with adaptation between successive stimulus applications. Due to its high temporal resolution, fTCD is useful for identifying quickly-evolving hemodynamic responses, and for correlating changes in hemodynamic parameters such as pulsatility index and CBFV.

Keywords

Ultrasonography; Doppler; Transcranial; Hemodynamics; Neuroprotection

Corresponding Author: Gregory R. Bashford, Address: 230 L.W. Chase Hall, East Campus, P.O. Box 830726, Lincoln, NE 68583-0726, gbashford2@unl.edu, Phone: (402) 472-1745, Fax: (402) 472-6338.

Disclosure

All other authors report no disclosures.

Introduction

Functional transcranial Doppler ultrasound (fTCD) is a technique which noninvasively measures changes in cerebral blood flow velocity (CBFV) in the major cerebral arteries during applied stimuli with high temporal resolution.[1] Changes in CBFV have been shown to be correlated with changes in cerebral blood flow (CBF) in the basal cerebral arteries if the arterial diameter remains constant, which appears to be a valid assumption under most conditions, for example hypercapnia and hypocapnia.[2] Through neurovascular coupling, changes in CBF in an artery may be related to activation of specific cortical areas within the territory perfused by that artery.[3]

As shown in rodent experiments, somatosensory stimulation (deflection of vibrissae) represents an intriguing possibility of protection from stroke by exploiting the plasticity of interactions between the cerebral cortex and its supporting vasculature.[4] Sensory stimulation was given to rats through stimulation of the whiskers, which possess large and detailed 'barrel' representations in the rodent cortex.[5] It has been suggested that similar neuroprotective effects might be created by sensory stimulation to the human hands or lips,[4] which possess similarly large and complex cortical representation.[6] Very few studies have directly measured the effect of sensory stimulation of the hands or lips on CBFV in the basal cerebral arteries,[7] although the effects of sensory stimulation of the hand on local or regional CBF have been studied by various modalities, including PET,[8,9] functional MRI (fMRI),[10–12] and functional near-infrared spectroscopy (fNIRS).[13] Each of these modalities has drawbacks and limitations. For example, PET has limited spatial[14] and temporal[8,15] resolution and involves radiation exposure,[16] fMRI has limited temporal resolution,[17] and fNIRS has relatively low spatial resolution.[18] The technique of fTCD provides a complement to these methodologies by allowing observation of CBFV changes within basal cerebral arteries non-invasively and in real time, with high temporal resolution (around 100 samples/s) at a single spatial point of observation in the basal artery. The observed CBFV changes derive from changes in the perfusion of the downstream territory of the basal artery under observation.[1]

A novel multichannel pneumotactile stimulation device has been developed by one of the authors.[10] In contrast with the electrical stimulation often used to study the CBF response to somatosensory stimuli,[19] pneumotactile stimulation is thought to provide recruitment of somatosensory nerve fibers in a more "natural" order than that provided by electrical stimulation.[6] Additionally, stimuli may be tuned to occur at a specific "traverse velocity" falling within an optimal range for evoking neural activation.[20] In this study, hemodynamic changes due to pneumotactile somatosensory stimulation at a specific traverse velocity of 25 cm/s were monitored in real time in the paired middle cerebral arteries using fTCD. The primary aim of this study was to determine the temporal characteristics and magnitude of changes in CBFV and other cerebral hemodynamic parameters in response to pneumotactile somatosensory stimulation in young, healthy adults.

Methods

Subjects

Twelve subjects between the ages of 19 and 27 (mean age: 23; 6M/6F) were recruited for this study. All were right-handed by the Edinburgh Handedness Inventory, with an average handedness score of 87% and range of 33–100%.[21] The procedure was approved by the Institutional Review Board of the University of Nebraska-Lincoln, and all subjects gave informed consent.

Equipment and Procedure

A transcranial Doppler ultrasound system (Doppler Box X, Compumedics Germany Gmbh, Singen, Germany) was used with 2 MHz pulsed-wave transducers to insonate the bilateral middle cerebral arteries (MCAs). The transducers were held on the subject's temporal acoustic window using a custom-made fixation device. The procedure for locating the MCAs and attaching the fixation device was as follows: first, a handheld transducer was used to locate the signal from each MCA. Next, the fixation device was placed on the subject, with the transducers positioned at the location found by handheld assessment. The MCAs were identified by their characteristic waveform, direction of flow (towards the transducer), and depth of signal (mean+/−std: 54.8+/−6.5 mm left, 57.3+/−5.3 mm right). For all but two subjects, the bifurcation of the carotid artery into the MCA and anterior cerebral artery was located on at least one side and served as a reference point for the location of the MCA (mean depth+/−std: 65.8+/−7.8 mm left (N = 9 subjects), 65.4 +/−3.7 mm right (N = 10 subjects)).

Somatosensory stimulation was applied using a Galileo tactile stimulus system developed by one of the authors (SB) (Epic Medical Concepts & Innovations, Olathe, KS, U.S.A.). An array of 14 custom-made miniature plastic air-filled capsules (TAC-Cells, 6 mm ID, Epic Medical Concepts & Innovations, Olathe, KS, U.S.A.) were adhered to the glabrous skin of the right hand with adhesive tape collars and tincture of Benzoin as shown in Fig. 1(B). Short (60 ms, 9.5 ms rise/fall) biphasic pressure pulses (+140 to −80 cmH_2O) were applied. These air pulses traversed the glabrous hand at a mean constant velocity of approximately 25 cm/s. The first pulse stimulated the distal phalanges for digits 2 through 5, followed sequentially by activation of cells placed on the middle phalanges for digits 2–5, metacarpals for digits 2–5, thenar eminence, and the distal phalanx of the thumb (digit 1). This saltatory stimulus train was cycled continuously for 20 s, which was followed by at least 5 minutes of rest (no stimulation). This stimulation-rest block was repeated three times for each subject (see Fig. 1(C) for experimental timeline).

Data Processing

The envelope data were processed using custom scripts in MATLAB R2014b (The Mathworks, Inc., Natick, MA, U.S.A.), following a previously described procedure.[1,22–24] Data were first visually inspected for poor signal or spurious peaks, and trials containing such data were not included in calculation of means (see below). Next, the left and right envelope waveform from each subject was filtered with a lowpass finite impulse response (FIR) filter (−1 dB at a passband frequency of f_{pass} = 0.47 Hz, −40 dB at a stopband

frequency of f_{stop} = 1.0 Hz, filter order = 266) to remove the quasi-cyclic effect of heart beat. Then, the filtered envelope waveforms were separated into individual trials, with each trial consisting of a baseline period (25 s), stimulus period (20 s), and rest period (3 min 30 s). The percent change dV(t)(%) was calculated for each trial as follows[1,23,24]:

$$dV(t)(\%) = 100\% * \frac{(V(t) - V_{pre.mean})}{V_{pre.mean}}, \quad (1)$$

where V(t) was the envelope waveform as a function of time and $V_{pre.mean}$ was the mean value of V(t) over the baseline period preceding the stimulus.

The percent change was then averaged over all trials for one subject to produce one graph of average percent change versus time for each subject. Finally, all subjects' data were averaged together to produce a plot of ensemble average percent change versus time for the envelope waveform data (Fig. 2(A)). Note that some trials were not included in ensemble averaging due to poor signal or spurious signal, as mentioned above; one subject had the second trial removed from both sides, and another subject had the second and third trials removed from both sides.

Lateralization ΔV(t) (%) was found by first finding the average percent change in envelope velocity for the left and right MCAs over all trials for each subject and then subtracting the right side from the left side, as follows[1,23,24]:

$$\Delta V(t)(\%) = dV(t)_{Left} - dV(t)_{Right}, \quad (2)$$

where $dV(t)_{Left}$ and $dV(t)_{Right}$ are the average percent change in the envelope velocity for the left side and right side as functions of time, as given from Equation (1). Positive values of ΔV(t) represent left lateralization while negative values represent right lateralization. All subjects' data were averaged together to produce a plot of ensemble average lateralization versus time for the envelope waveform data (Fig. 2(B)).

Systolic (V_s) and diastolic (V_d) velocities were found per heartbeat from the unfiltered envelope velocity data using a custom MATLAB script. The mean velocity (V_m) per heartbeat was then found by numerically integrating the unfiltered envelope velocity waveform from the time of one V_s to the time of the next V_s, divided by the time length of the cycle. Finally, pulsatility index (PI), a measure of distal arterial resistance,[25] was calculated for each heartbeat using the following equation[26]:

$$PI_i = \frac{V_{s,i} - V_{d,i}}{V_{m,i}}, \quad (3)$$

where subscript i denotes ith heartbeat, PI_i is the value of PI, $V_{s,i}$ is the systolic velocity, $V_{d,i}$ is the diastolic velocity, and $V_{m,i}$ is the mean velocity. For time synchronization purposes,

the time of PI_i was taken as the time of $V_{s,i}$ for each heartbeat. A linear interpolation function in MATLAB was used to interpolate PI_i values between heartbeats, followed by sampling at 100 Hz to create a uniform time base[27] and allow for averaging across trials and subjects. The percent change versus time for PI was calculated for each trial and then averaged across all trials and all subjects, using the same procedure as given above for the envelope waveform.

Statistics

To test whether the maximum evoked response decreased with successive stimuli, ensemble averages were calculated for the first, second, and third trials separately for envelope velocity and lateralization. Only data from the ten subjects with no discarded trials (see above) were used, to avoid using incomplete blocks. SAS v9.4 software (SAS Institute, Inc., Cary, NC, U.S.A.) was used to compare between the trials to see if adaptation was occurring. First, the time t_{max} at which the largest percent change occurred for each trial was found. Next, a custom MATLAB script was used find the average of each trial over a 0.5 s time interval centered at t_{max}. This averaging was performed for each subject and each side individually. Finally, the averages for all subjects were input into SAS and analyzed using analysis of variance (ANOVA), with blocking by subjects, blocks treated as random, and Tukey correction for multiple comparisons. Upper and lower limits for 95% confidence intervals were calculated using lsmeans in SAS.

Results

Figure 2(A) shows the ensemble average envelope velocity percent change versus time. Initially, both sides have a maximum evoked increase of about 13.3% at 3.5 s after stimulation begins (iv). Envelope velocity falls below 0% (vi) and rises again (ix). Envelope velocity has a brief latency after the stimulus ends (xi) before returning to 0% (xiii). There is an undershoot at about 38 s after stimulation ends (xv). Because the envelope velocity remains close to 0% for the remainder of the rest period, the last 95 s of the rest period are not shown.

Figure 2(B) shows ensemble average PI percent change versus time. PI decreases initially, reaching a minimum at 3.4 s after stimulation begins (iv). PI then rises (vi), staying elevated until 18 s after stimulus onset, and then begins to fall (viii), reaching 0% about 18 s after stimulus removal (xiii). There is a brief increase in PI at about 28 s after stimulation ends (xiv), and PI then remains close to 0%, with small variations. The last 95 s of the rest period are not shown.

Figure 2(C) shows the ensemble average lateralization versus time. There is a left-lateralized peak during the baseline period (i). When the stimulus begins, lateralization rises quickly, reaching a maximum left lateralization of 2.0% about 16 s after stimulus onset (vii). After the stimulus ends, there is a minimum (right) lateralization of −1.5% (x). Lateralization returns to 0% (xii) and has moderate variations about 0% for the remainder of the rest period. However, the variation occurs over short time periods, suggesting that random fluctuations are the cause. The last 95 s of the rest period are not shown.

Plots of the ensemble average envelope velocity percent change versus time for the first, second, and third trials are shown in Figs. 3(A) and 3(B), illustrating adaptation effects. The maximum percent change for the first trial, occurring at about 3.6 s after stimulus onset, has a magnitude of 20.5% on the left side and 18.8% on the right side. The maximum percent change for the second trial is 13.8% on the left side and 13.4% on the right side, and the maximum percent change for the third trial is 9.2% on the left side and 6.6% on the right side.

A plot of the ensemble average lateralization versus time for the first, second, and third trials is shown in Fig. 3(C). The maximum lateralization for the first trial occurs at about 18.4 s after stimulus onset with a value of 3.9%. The maximum lateralization for the second trial occurs at about 16.0 s after stimulus onset with a value of about 3.3%, and the maximum lateralization for the third trial occurs at about 7.8 s after stimulus onset with a value of about 2.6%.

Table 1 shows upper limits, lower limits, and p-values for the Tukey-corrected 95% confidence intervals for differences between the maximum percent changes in ensemble average envelope velocity for pairs of trials. Table 2 shows the upper limits, lower limits, and p-values for the 95% confidence intervals for the maximum lateralization for each trial.

Discussion

Most notably, the large, sharp increase in the ensemble average envelope velocity during the first trial (Fig. 3) indicates that a large, rapid neuronal activation is evoked by pneumotactile somatosensory stimulation. This increase is comparable to that seen with the most potent stimuli studied with fTCD, such as visual stimuli, which may lead to a 40% increase in CBFV in the posterior cerebral artery,[28] and breath holding, which may lead to a 30% or greater increase in CBFV in the MCA.[29] In this experiment, the full hand was stimulated with a saltatory (“moving”) stimulus traveling at a traverse velocity anticipated to create a maximum neural response[20]; a large percent increase in CBFV would be expected for such a potent stimulus. For the first trial alone, the maximum percent increase in the ensemble average envelope velocity is 20%, and averaging across 3 trials, the maximum percent increase in the envelope velocity is 13.3% for the first peak and 5.8% for the second peak.

Figure 2 highlights the ability of fTCD to provide high temporal resolution information on changes in correlated hemodynamic variables. For example, while the ensemble average envelope velocity (Fig. 2(A)) initially increases to a maximum at 3.5 s after stimulation onset, the PI (Fig. 2(B)) simultaneously decreases (Table 3, row iv). Since PI is a measure of distal arterial resistance,[25] the initial sharp increase in ensemble average envelope velocity is likely due to a rapid decrease in resistance via vasodilation of arteries distal from the MCA. However, ensemble average PI does not decrease during the second maximum in the ensemble average envelope velocity (about 3.4 s after stimulation end), possibly due to greater between-subject variance for PI during this second rise in envelope velocity.

Adaptation effects can be seen when looking at the sharp initial increase in the ensemble average envelope velocity percent change (Figs. 3(A)–(B)). For both sides, the maximum

percent change in the first trial is significantly different from that in the third trial (Table 1), indicating some decrease during repeated applications of the stimulus. However, the maximum percent change in the first trial is not significantly different from that in the second trial, and the maximum percent change in the second trial is not significantly different from that in the third trial. An exponential model of the form

$$dV_{max}(k) = Ae^{-bk}, \quad (4)$$

where A and b are positive constants, fits a scatterplot of the data for maximum percent change for each subject, $dV_{max}(k)$, versus the trial number minus one (k), with $r^2 = 0.216$ for the left side and $r^2 = 0.162$ for the right side (not shown). However, when exponential models of the form given in Eqn. 4 are fit to individual subjects' data, r^2 values are higher, with 7 of 10 subjects having $r^2 > 0.6$. A decreasing exponential trend is a known characteristic of adaptation (or "habituation"), which is the process by which the brain adapts to repeated stimuli.[30] Adaptation is present at all levels from mechanoreceptors to relays in the central nervous system,[31] and has previously been observed in humans[31] and anesthetized animals.[32] The peak occurring 3.5 s after stimulus onset in the ensemble average envelope velocity versus time plot (Fig. 2(A)) appears to adapt quickly with subsequent trials, while the second, lower peak beginning 9.6 s after stimulus onset may represent a more "steady-state" response to pneumotactile stimulation. Due to its high temporal resolution, the technique of fTCD may thus be very useful for identifying quickly-evolving responses such as the first peak in Fig. 2(A), which would likely be missed by other functional imaging modalities.

Slight left lateralization, contralateral to the stimulus, occurs during stimulation (Fig. 2(C)), similar to what has been observed in other tactile somatosensory stimulation experiments (see Introduction). Lateralization may slightly decrease over successive trials; although no trials are significantly different from the others, only the first and second trials have a maximum lateralization that is significantly different from 0% (Table 2). The maximum ensemble average lateralization reaches 3.9% during the first trial (Fig. 3(C)) and 2.0% when averaged over all three trials (Fig. 2(C)). Although small, this value of lateralization is similar in magnitude to other fTCD literature values during various stimuli, including visuospatial tasks[22] and word generation tasks.[23,24,33] Due to interhemispheric connections and the highly distributed nature of the somatosensory system,[34] the neural response is distributed throughout both hemispheres. The bilateral response to unilateral pneumotactile somatosensory stimulation has been observed previously using fMRI,[10] and may explain the small overall lateralization observed.

In this preliminary study, subjects were recruited from a young and healthy population without any known neurological deficits or disorders. Both age and vascular health might affect the results obtained, however. For example, the maximum percent increase in the envelope velocity might be smaller for older subjects, who have been shown to have a decreased evoked CBFV response to visual stimuli compared to younger subjects.[28] Also, older populations are more likely to have diseased vasculature, for example carotid artery

atherosclerosis,[35] which may affect the ability of the vasculature to respond to neural stimuli.[36]

The aim of the present study was to characterize the hemodynamic response to pneumotactile somatosensory stimulation using fTCD. Results showed a large cerebral neuronal activation in response to tactile stimulation of the hand, with up to a 20% increase in CBFV, demonstrating the potency of the saltatory pneumotactile stimulation of the hand. Changes in MCA envelope velocity during stimulation appeared to correspond with changes in distal arterial resistance, as measured by the pulsatility index. The maximum percent change in the ensemble average envelope velocity decreased over successive trials, showing adaptation. Slight left lateralization appeared to occur during pneumotactile stimulation of the right hand, as expected physiologically. These results show that the pneumotactile somatosensory stimulation can augment cerebral blood flow, and its potential to induce plastic changes in the brain's neurovasculature and provide protection from ischemic stroke should be explored further.

Acknowledgments

The authors thank AnnaJean Scarborough for help with subject recruitment, Mohammed Alwatban for help with statistical analysis, Jake Greenwood for help with programming, Aria Tarudji for help with figure preparation, and Edward Truemper for mentorship. This work was partially supported by a grant from the Eunice Kennedy Shriver National Institute of Child Health and Human Development NICHD R01-HD086088 and the Barkley Trust Foundation (Steven Barlow – PI), and by the Nebraska Agricultural Experiment Station with funding from the Hatch Act (Accession Number 1002348) through the USDA National Institute of Food and Agriculture. Dr. Barlow is the principal inventor of the Galileo which is licensed to Epic Medical Concepts & Innovations (Mission, KS, USA) by the University of Kansas and the University of Nebraska.

References

1. Deppe M, Ringelstein EB, Knecht S. The investigation of functional brain lateralization by transcranial Doppler sonography. Neuroimage. 2004; 21:1124–46. [PubMed: 15006680]
2. Serrador JM, Picot PA, Rutt BK, Shoemaker JK, Bondar RL. MRI measures of middle cerebral artery diameter in conscious humans during simulated orthostasis. Stroke. 2000; 31:1672–8. [PubMed: 10884472]
3. Huneau C, Benali H, Chabriat H. Investigating human neurovascular coupling using functional neuroimaging: a critical review of dynamic models. Front Neurosci. 2015; 9:467. [PubMed: 26733782]
4. Lay CC, Davis MF, Chen-Bee CH, Frostig RD. Mild sensory stimulation completely protects the adult rodent cortex from ischemic stroke. PLoS One. 2010; 5:e11270. [PubMed: 20585659]
5. Petersen CC. The functional organization of the barrel cortex. Neuron. 2007; 56:339–55. [PubMed: 17964250]
6. Hlustik P, Solodkin A, Gullapalli RP, Noll DC, Small SL. Somatotopy in human primary motor and somatosensory hand representations revisited. Cereb Cortex. 2001; 11:312–21. [PubMed: 11278194]
7. Sitzer M, Knorr U, Seitz RJ. Cerebral hemodynamics during sensorimotor activation in humans. J Appl Physiol. 1994; 77:2804–11. [PubMed: 7896625]
8. Fox PT, Raichle ME. Focal physiological uncoupling of cerebral blood flow and oxidative metabolism during somatosensory stimulation in human subjects. Proc Natl Acad Sci USA. 1986; 83:1140–4. [PubMed: 3485282]
9. Greenberg JH, Reivich M, Alavi A, et al. Metabolic mapping of functional activity in human subjects with the [18F]fluorodeoxyglucose technique. Science. 1981; 212:678–80. [PubMed: 6971492]

10. Oh H, Custead R, Wang Y, Barlow S. Neural encoding of saltatory pneumotactile velocity in human glabrous hand. PLoS One. 2017; 12:e0183532. [PubMed: 28841675]
11. Maldjian JA, Gottschalk A, Patel RS, Detre JA, Alsop DC. The sensory somatotopic map of the human hand demonstrated at 4 Tesla. Neuroimage. 1999; 10:55–62. [PubMed: 10385581]
12. Pfannmoeller JP, Greiner M, Balasubramanian M, Lotze M. High-resolution fMRI investigations of the fingertip somatotopy and variability in BA3b and BA1 of the primary somatosensory cortex. Neuroscience. 2016; 339:667–77. [PubMed: 27777015]
13. Rosner AO, Barlow SM. Hemodynamic changes in cortical sensorimotor systems following hand and orofacial motor tasks and pulsed pneumotactile stimulation. Somatosens Mot Res. 2016; 33:145–55. [PubMed: 27550186]
14. Fox PT, Raichle ME. Stimulus rate dependence of regional cerebral blood flow in human striate cortex demonstrated by positron emission tomography. J Neurophysiol. 1984; 51:1109–20. [PubMed: 6610024]
15. Aaslid R. Visually evoked dynamic blood flow response of the human cerebral circulation. Stroke. 1987; 18:771–5. [PubMed: 3299883]
16. Towson JEC. Radiation dosimetry and protection in PET. In: Valk PE, Bailey DL, Townsend DW, Maisey MN, editorsPositron Emission Tomography: Basic Science and Clinical Practice. London: Springer-Verlag London Ltd; 2003. 265–79.
17. Buxton RB. The physics of functional magnetic resonance imaging (fMRI). Rep Prog Phys. 2013; 76:096601. [PubMed: 24006360]
18. Bunce SC, Izzetoglu M, Izzetoglu K, Onaral B, Pourrezaei K. Functional near-infrared spectroscopy: an emerging neuroimaging modality. IEEE Eng Med Biol Mag. 2006; 25:54–62.
19. Liao LD, Bandla A, Ling JM, et al. Improving neurovascular outcomes with bilateral forepaw stimulation in a rat photothrombotic ischemic stroke model. Neurophotonics. 2014; 1:011007. [PubMed: 26157965]
20. Whitsel BL, Franzen O, Dreyer DA, et al. Dependence of subjective traverse length on velocity of moving tactile stimuli. Somatosens Res. 1986; 3:185–96. [PubMed: 3749661]
21. Oldfield RC. The assessment and analysis of handedness: the Edinburgh inventory. Neuropsychologia. 1971; 9:97–113. [PubMed: 5146491]
22. Hage B, Alwatban MR, Barney E, et al. Functional transcranial Doppler ultrasound for measurement of hemispheric lateralization during visual memory and visual search cognitive tasks. IEEE Trans Ultrason Ferroelectr Freq Control. 2016; 63:2001–7. [PubMed: 27576247]
23. Knecht S, Deppe M, Ringelstein EB, et al. Reproducibility of functional transcranial Doppler sonography in determining hemispheric language lateralization. Stroke. 1998; 29:1155–9. [PubMed: 9626288]
24. Knecht S, Deppe M, Ebner A, et al. Noninvasive determination of language lateralization by functional transcranial Doppler sonography: a comparison with the Wada test. Stroke. 1998; 29:82–6. [PubMed: 9445333]
25. Petersen LJ, Petersen JR, Talleruphuus U, Ladefoged SD, Mehlsen J, Jensen HA. The pulsatility index and the resistive index in renal arteries. Associations with long-term progression in chronic renal failure. Nephrol Dial Transplant. 1997; 12:1376–80. [PubMed: 9249772]
26. Gosling RG, King DH. Arterial assessment by Doppler-shift ultrasound. Proc R Soc Med. 1974; 67:447–9. [PubMed: 4850636]
27. Salinet AS, Robinson TG, Panerai RB. Cerebral blood flow response to neural activation after acute ischemic stroke: a failure of myogenic regulation? J Neurol. 2013; 260:2588–95. [PubMed: 23824356]
28. Panczel G, Daffertshofer M, Ries S, Spiegel D, Hennerici M. Age and stimulus dependency of visually evoked cerebral blood flow responses. Stroke. 1999; 30:619–23. [PubMed: 10066861]
29. Markus HS, Harrison MJ. Estimation of cerebrovascular reactivity using transcranial Doppler, including the use of breath-holding as the vasodilatory stimulus. Stroke. 1992; 23:668–73. [PubMed: 1579964]
30. Thompson RF, Spencer WA. Habituation: a model phenomenon for the study of neuronal substrates of behavior. Psychol Rev. 1966; 73:16–43. [PubMed: 5324565]

31. Venkatesan L, Barlow SM, Popescu M, Popescu A. Integrated approach for studying adaptation mechanisms in the human somatosensory cortical network. Exp Brain Res. 2014; 232:3545–54. [PubMed: 25059913]

32. Prosser CL, Hunter WS. The extinction of startle responses and spinal reflexes in the white rat. Am J Physiol. 1936; 117:609–18.

33. Knecht S, Henningsen H, Deppe M, Huber T, Ebner A, Ringelstein EB. Successive activation of both cerebral hemispheres during cued word generation. Neuroreport. 1996; 7:820–4. [PubMed: 8733753]

34. Aronoff R, Matyas F, Mateo C, Ciron C, Schneider B, Petersen CC. Long-range connectivity of mouse primary somatosensory cortex. Eur J Neurosci. 2010; 31:2221–33. [PubMed: 20550566]

35. Fabris F, Zanocchi M, Bo M, et al. Carotid plaque, aging, and risk factors: a study of 457 subjects. Stroke. 1994; 25:1133–40. [PubMed: 8202970]

36. Ances BM, Greenberg JH, Detre JA, Dietrich WD. Acute carotid occlusion alters the activation flow coupling response to forepaw stimulation in a rat model. Stroke. 2000; 31:955–60. [PubMed: 10754005]

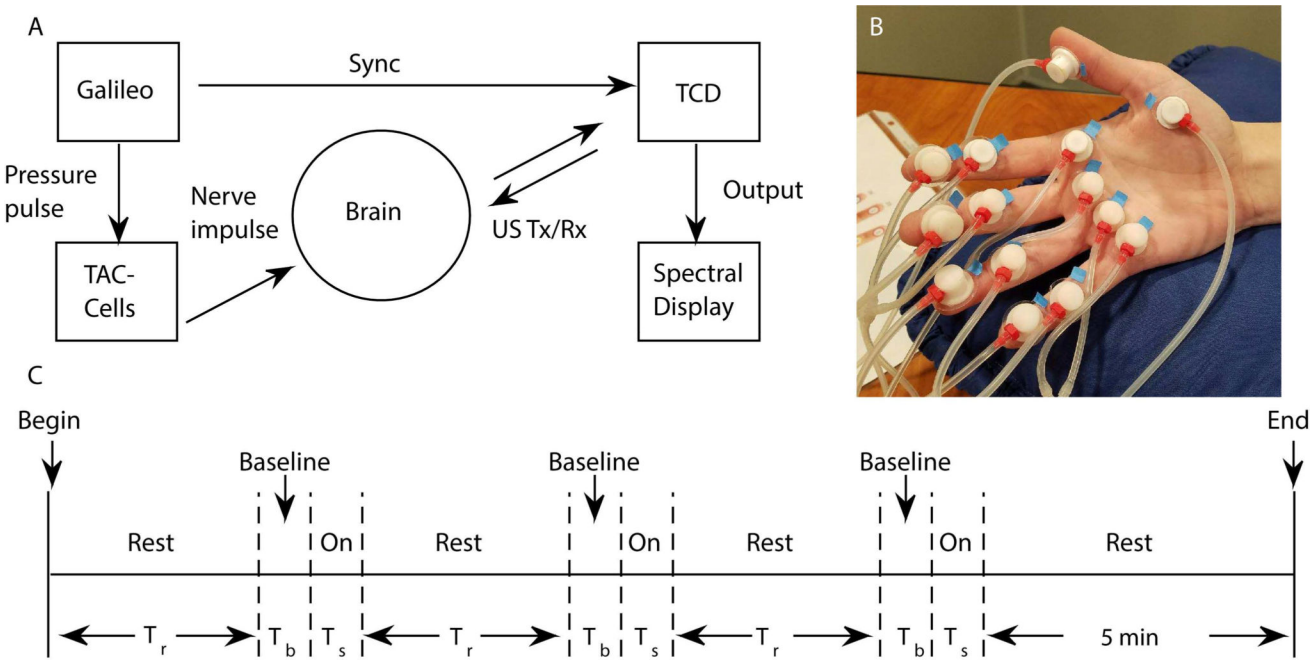

Fig. 1. Experimental Setup and Timeline

(A) Experimental setup. US Tx/Rx = ultrasound transmitted/received pulse, Sync = synchronization signal. (B) Hand with TAC-cells. (C) Timeline of experiment. Rest time (T_r) = 4 min 35 s, baseline time (T_b) = 25 s, and stimulus time (T_s) = 20 s.

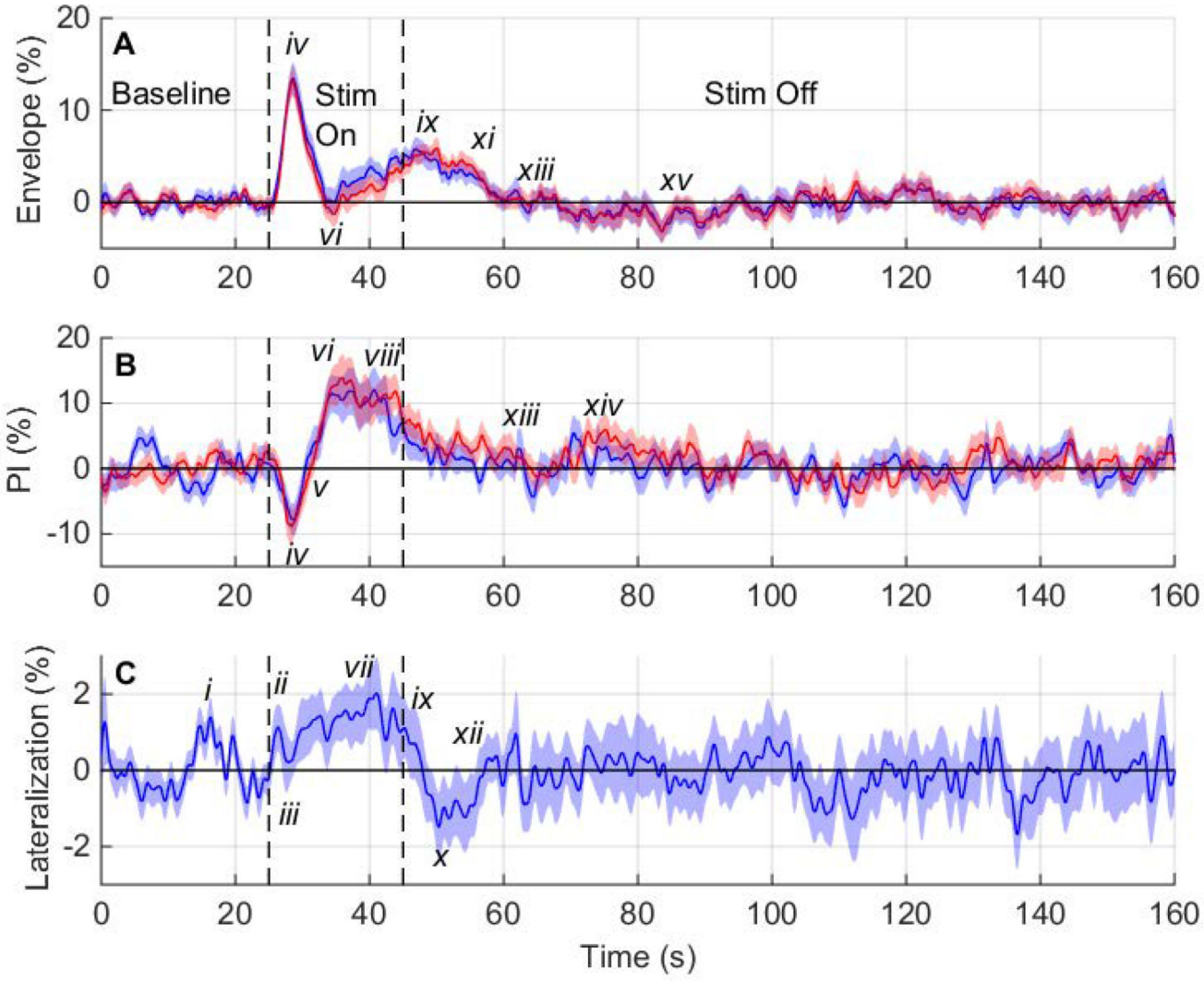

Fig. 2. Percent Change in Hemodynamic Variables vs. Time for 12 Subjects

(A) Plot of the ensemble average percent change in the envelope velocity versus time for the left (blue) and right (red) middle cerebral arteries (MCAs), (B) plot of the ensemble average percent change in the pulsatility index versus time for the left (blue) and right (red) MCAs, and (C) plot of the ensemble average lateralization versus time. Shaded regions indicate the standard error of the mean (n = 33 trials). Stim = stimulus, PI = pulsatility index.

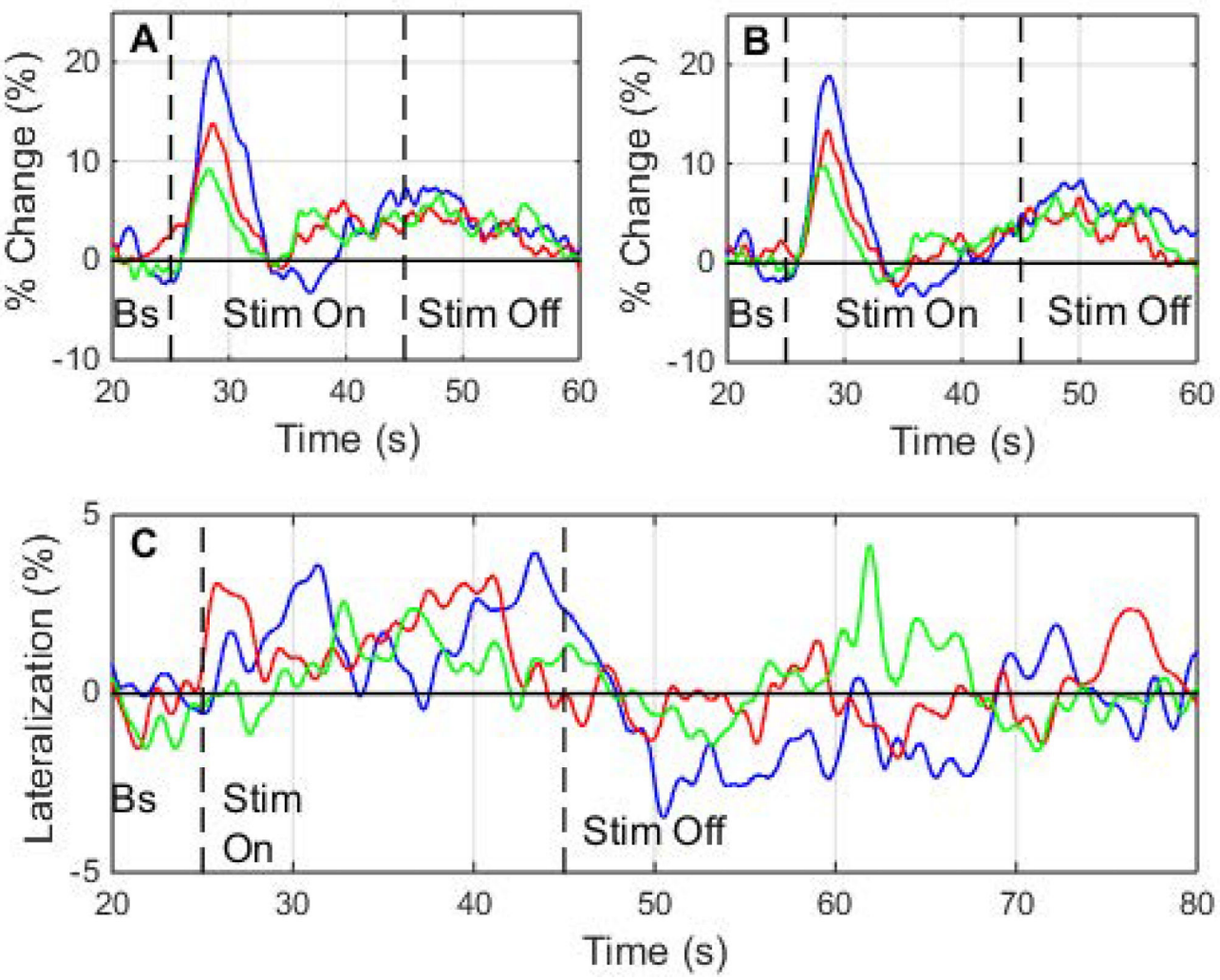

Fig. 3. Adaptation vs. Time in Envelope Velocity and Lateralization

Plot of ensemble average envelope velocity percent change versus time for each trial, showing adaptation occurring between trials, for the (A) left side and (B) right side. (C) Plot of lateralization versus time for each trial. Error bars not shown for clarity. Bs = baseline, Stim = stimulus.

Table 1

Comparison of Maximum Percent Change of Envelope Velocity for Each Trial

Results of an analysis of variance comparing the maximum percent change of envelope velocity of each consecutive trial, showing upper and lower limits of the Tukey-corrected 95% confidence interval, and the p-value.

	Left Side			Right Side		
Comparison	**Lower**	**Upper**	**p-value**	**Lower**	**Upper**	**p-value**
1 versus 2	−1.95	15.53	0.1452	−2.72	13.94	0.2259
1 versus 3	2.55	20.03	0.0106*	0.76	17.43	0.0313*
2 versus 3	−4.24	13.24	0.4058	−4.85	11.82	0.5461

Starred values are statistically significant at the 0.05 alpha level.

Table 2
aximum Lateralization Value for Each Trial

Results of an analysis of variance comparing the maximum lateralization value during stimulation to zero lateralization, showing upper and lower limits of the 95% confidence interval.

Trial	Lower	Upper	p-value
1	0.66	7.12	0.0210 *
2	0.01	6.47	0.0496 *
3	−0.74	5.72	0.1234

Starred values are statistically significant at the 0.05 alpha level.

Table 3
Time Points and Percent Change Values for Figure 2

Time points and values of ensemble average percent change in envelope velocity, ensemble average percent change in pulsatility index (PI), and ensemble average lateralization, at points corresponding to small Roman numerals in Fig. 2. For envelope velocity and PI, time points and percent change are averages of left and right sides. Time is measured from beginning of stimulation. (A), (B), and (C) refer to the corresponding subfigures in Fig. 2

Marker	Time (s)	% Change (%)
i	−3.8	1.4
ii	1.4	1.1
iii	2.9	0.2
iv	3.6(A), 3.4(B)	13.3(A), −8.3(B)
v	5.8	0.0
vi	9.6(A), 9.5(B)	−0.65(A), 12.0(B)
vii	16.1	2.0
viii	18.0	11.3
ix	23.4(A), 22.9(C)	5.8(A), 0.0(C)
x	25.3	−1.5
xi	30.1	3.6
xii	32.1	0.0
xiii	36.6(A), 37.8(B)	0.0(A), 0.0(B)
xiv	47.8	5.7
xv	58.6	−3.2